

Design of ANSI S1.11 Filter Bank for Digital Hearing Aids

Yu-Ting Kuo, Tay-Jyi Lin, Yueh-Tai Li, Wei-Han Chang, and Chih-Wei Liu
Department of Electronics Engineering, National Chiao Tung University, Taiwan

Shuenn-Tsong Young

Institute of Biomedical Engineering, National Yang-Ming University, Taiwan

Abstract – Existing digital hearing aids, to our knowledge, all exclude ANSI S1.11-compliant filter banks because of the high computational complexity. Most ANSI S1.11 designs are IIR-based and only applicable in applications where linear phase is not important. This paper presents an FIR-based ANSI S1.11 filter bank for digital hearing aids, which adopts a multi-rate architecture to reduce the data rates on the bandwidth-limited bands. A systematic way is also proposed to minimize the FIR orders thereof. In an 18-band digital hearing aid with 24 kHz input sampling rate, the proposed design with linear phase has comparable computational complexity with IIR filter banks. Moreover, our design requires only 4% multiplications and additions of a straightforward FIR implementation.

I. INTRODUCTION

The small dimension of hearing aids severely limits the sizes of electronic devices and battery (thus the power consumption of the devices). Hence, designers must try their best to reduce the algorithmic complexity first to meet the crucial area and power constraints. Fig. 1 depicts a generic digital hearing aid, including functional blocks such as auditory compensation, echo (feedback) cancellation, noise reduction/suppression, and speech enhancement, etc. Auditory compensation is the main function in hearing aids, which performs frequency shaping to compensate the hearing loss. A filter bank decomposes the input signal into different frequency bands so that the prescribed gains can be applied on each band. A compressor then compresses dynamic ranges of the compensated signals to fit the diminished dynamic range of the hearing impaired.

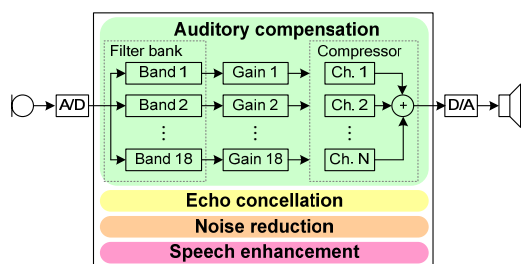


Figure 1. Digital hearing aid

A fitting procedure calculates the individual gains to be applied on each band, and most fitting procedures (e.g. NAL-NL1 [1][2]) are based on 1/3-octave bands. ANSI S1.11 standard [3] defines the

specification for the octave and fractional-octave band filters for acoustics applications. However, most hearing aids use proprietary filter banks instead to reduce the implementation complexity [4][5], which do not comply with the ANSI S1.11 standard. By the way, existing ANSI S1.11 implementations [6][7], to our knowledge, are all based on IIR filters, even in applications with more budgets on silicon area and power consumption. Unfortunately, linear phase is essential in feedback cancellation [4], which is another important building block in digital hearing aids. In other words, IIR is not feasible. Therefore, a low-complexity FIR filter bank that complies with the ANSI S1.11 standard is desired for digital hearing aids. In this paper, we propose a multi-rate FIR filter bank to minimize data rates of the bandwidth-limited bands. We also propose a systematic method to synthesize the minimal FIR coefficients for the multi-rate filter bank.

The rest of this paper is organized as follows. Section 2 describes the 1/3-octave bands briefly and reviews the ANSI S1.11 specification. Section 3 shows the adopted multi-rate architecture for the 1/3-octave filter bank and our proposed flow for the design and optimization of the FIR coefficients thereof. The comparisons of the computational complexity and the filter response of our proposed approach are summarized in Section 4. Finally, Section 5 concludes this paper and outlines our future researches.

II. ANSI S1.11 SPECIFICATION

ANSI S1.11 provides the performance specification for the octave and fractional-octave-band filter bank. This section would briefly describe the definition of the 1/3-octave bands and the performance requirement of ANSI S1.11 filter banks.

A. 1/3-octave Bands

ANSI standard defines 43 1/3-octave bands in the frequency range of 0~20 KHz. Each band's location and range is specified by its mid-band frequency and bandwidth. The mid-band frequency of the x^{th} band $f_m(x)$ is defined as

$$f_m(x) = 2^{\frac{(x-30)}{3}} \times f_r,$$

where f_r is the reference frequency set as 1,000 Hz in the standard. For example, the mid-band frequency of the 29th band $f_m(29)$ is 794 ($= 2^{\frac{(29-30)}{3}} \times 1,000$), and the mid-band frequency of the 31st band $f_m(31)$ is 1,260 ($= 2^{\frac{(31-30)}{3}} \times 1,000$). Besides, the standard defines each band's lower (f_1) and upper (f_2) band-edge frequencies as

$$f_1 = f_m \times 2^{-\frac{1}{6}}, f_2 = f_m \times 2^{\frac{1}{6}}$$

The bandwidth is defined as the frequencies between f_1 and f_2 . For instance, the bandwidth of the 30th band is from 891 Hz to 1,112 Hz.

B. Performance Requirement

ANSI S1.11 standard describes the specifications of the filter's relative attenuation, integrated filter response, environment sensitivity (e.g. humidity, electromagnetic field, and temperature), maximum output signal, terminating impedance and some other parameters for three filter classes, that is, class-0, 1, and 2. The specification of the relative attenuation for class-2 filters is shown in Fig. 2, where the green and red curves respectively represent the limits on the maximum and the minimum attenuations. Fig 2 shows that a class-2 filter allows a 1 dB ripple in its passband region (i.e. $f_1 \sim f_2$) and has a 60 dB attenuation at frequencies small than f_1' ($= f_m \times 0.184$) and at frequencies greater than f_2' ($= f_m \times 5.434$). The specifications of class-0 and class-1 filters are stricter than that of class-2 filters. For example, the maximum passband ripple of class-1 filters is 0.6 dB. This paper design an 18-band filter bank for the 22nd ~ 39th band (covering the frequency from 140 Hz to 8980 Hz) with the class-2 specifications.

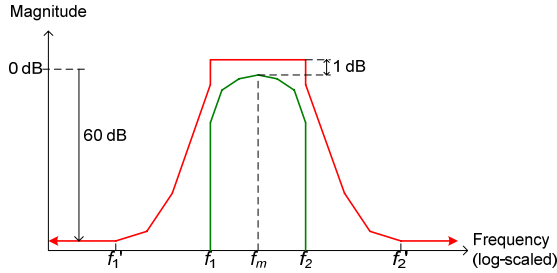


Figure 2. ANSI S1.11 class-2 filter specification

III. PROPOSED ARCHITECTURE AND FILTER DESIGN

In this section, we describe the 1/3-octave filter bank design that comply with the ANSI S1.11 class-2 specification for a digital hearing aid with 18-band auditory compensation [9].

A. Filter Bank Architecture

Fig. 3 shows the proposed multi-rate architecture of the 18-band filter bank, where the symbol X and Y denote the input and output of the auditory compensation respectively. The multi-rate filter bank only implements the highest octave's three filters (i.e. F_{37} , F_{38} and F_{39}) and a decimation filter (denoted by D). In the rest of this paper, we use the notation F_n to represent the filter of the n th band.

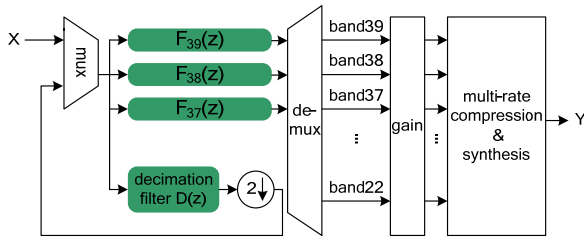


Figure 3. Proposed filter bank architecture

According to the 1/3-octave definition, each octave (i.e. three 1/3-octave bands) has the identical frequency characteristics if the sampling rate is reduced by 2 for every octave. For example, the characteristics of the 36th band are the same as that of the 39th band if its sampling rate is half of that of the 39th band. Therefore, our multi-rate filter bank could iteratively calculate the lower octaves with $F_{37} \sim F_{39}$, when the input signal is band-limited by D and down-sampled by 2 for each octave, as shown in Fig. 3. This implies that we need not to design extremely narrow-band filters (which require high-order FIR) for the lowest octave bands

The proposed multi-rate filter bank minimizes the sampling rate of the band-limited channels to reduce the computation complexity of the filter bank and the compressor. However, a synthesis block is required to up-sample those channels before output. The equivalent datapaths for the 39th, 36th, and 33rd bands is depicted in Fig. 4, where the symbol I denotes the interpolation filter and Y_n denotes the n th band's output. The sampling rate of the compression block is reduced to the half in the 36th band, and one fourth in the 33rd band. Besides, the signal in the 39th band is also band-limited by F_{39} such that the compression of the 39th band could operate at a lower sampling rate. Hence, there might be additional decimators in the compression block to further reduce the sampling rate. However, we focus our discussion on the filter bank and the details of the compressor are beyond this paper's scope.

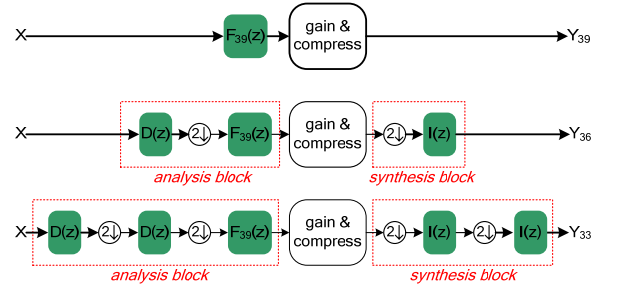


Figure 4. Datapath of the 39th, 36th and 33rd bands

To derive each band's response, we first remove the gain & compress block from the datapath for simplicity. The simplified datapath of the 36th band is shown in Fig. 5(a), where we could exploit the noble identity [8] such that F_{39} is moved to the front of the decimator, as shown in Fig. 5(b).

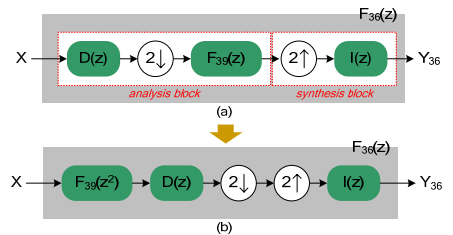


Figure 5. (a) Simplified datapath of the 36th band, (b) noble identity

The multi-rate processing in Fig. 5(b), that is, the function of $D(z)$, down-sampled by 2, up-sampled by 2, and $I(z)$ is described as $\frac{1}{2}X(z) \cdot D(z) \cdot I(z) + \frac{1}{2}X(-z) \cdot D(-z) \cdot I(z)$ [8]. Therefore, we could write the equation of Y_n ($n = 22 \sim 36$) as

$$Y_n(z) = \frac{1}{2} [X(z) \cdot F_{n+3}(z^2) \cdot D(z) \cdot I(z)] + \frac{1}{2} [X(-z) \cdot F_{n+3}(z^2) \cdot D(-z) \cdot I(z)] \quad (1)$$

B. Filter Design

The FIR coefficients are designed using MATLAB `firpm` and `firpmord` functions. `firpmord` uses the parameters shown in Fig. 6 to generate the required inputs (such as filter order) for `firpm`, which then uses the results of `firpmord` to produce the filter coefficients. In other words, we need to find out the optimal values of the parameters (i.e. $fs1$, $fp1$, $fp2$ and $fs2$) in Fig. 6 for F_{37} , F_{38} , F_{39} , D and I respectively. Note that only one passband frequency and one stopband frequency need to be specified when we design low-pass filters.

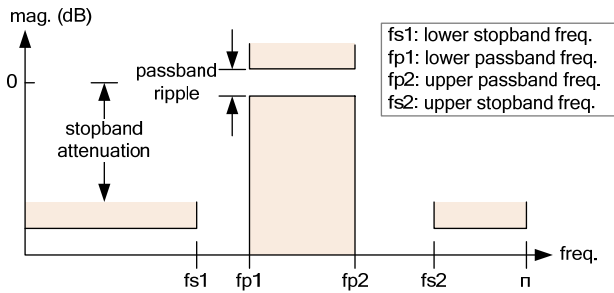


Figure 6. Parameters of the `firpmord` function in MATLAB

The filter design problem for the multi-rate filter banks is to find the coefficients of F_{37} , F_{38} , F_{39} , D and I , so that $F_{22} \sim F_{39}$ meet ANSI S1.11 class-2 specification and the overall computational complexity is minimized. A filter design flow that contains two steps is proposed. The following will describe the details of our filter design flow.

■ Step 1: Design $F_{37} \sim F_{39}$ and D/I independently

We first design $F_{37} \sim F_{39}$ such that the specifications of the 37th~39th bands are met and the orders are minimized. Following the ANSI S1.11 class-2 specification shown in Fig. 2, the passband ripple and stopband attenuation of $F_{37} \sim F_{39}$ are set as 1 and 60 dB respectively. In other words, we need to find out the optimal values of $fs1$, $fp1$, $fp2$ and $fs2$ for $F_{37} \sim F_{39}$. Since the orders of the designed filters are dominated by the filters' transition bandwidths, the problem of finding $fs1$, $fp1$, $fp2$ and $fs2$ is then translated into finding the transition bandwidths (denoted as TBW1 and TBW2), $fs1$ and $fs2$, where $TBW1 = fp1 - fs1$ and $TBW2 = fs2 - fp2$. Besides, to simplify the design process, we decompose the band-pass filter specifications of $F_{37} \sim F_{39}$ into a low-pass and a high-pass specifications and find the range of TBW1 and TBW2 separately. That is, we try to design a high-pass filter satisfying the high-pass specification with the transition bandwidth = TBW1, and a low-pass filter satisfying the low-pass specification with the transition bandwidth = TBW2. The range of TBW is determined as following: we first find the widest TBW (with which the designed filter could satisfy the high-pass/low-pass specification) and its corresponding order (denoted as `ord_min`), then we find the narrowest TBW with comparable order (i.e. `order < ord_min * 1.1`). We then check the feasibility of the TBW pairs (i.e. verify that the band-pass filter design with certain TBW pair could meet the specification) and

select the best results among those feasible TBW pairs. In this step, F_{37} , F_{38} and F_{39} are designed as 40-tap, 33-tap, and 25-tap filters, respectively.

Secondly, we design D and I assuming that the magnitude of $F_{37} \sim F_{39}$ is 0 dB for frequencies between f_1 and f_2 (which are defined in Section 2), while the magnitude is -60 dB for other frequencies. Under this assumption, the attenuation of $F_{22} \sim F_{35}$ would meet the specifications as long as F_{36} meets (but not including ripple). Therefore, we consider the equation of Y_{36} , which can be found in (1) with $n = 36$. We ignore the scalar constant $1/2$ and assume the aliasing term $X(-z)$ is to be suppressed; thus the response of F_{36} is $F_{39}(z^2) \cdot D(z) \cdot I(z)$. That is, $D(z)I(z)$ should be a low-pass filter which suppresses the image in $F_{39}(z^2)$ and $D(z)I(z)$'s ripple should be small enough so that the ripples of $F_{22} \sim F_{36}$ are within 1 dB. Besides, $D(-z)I(z)$ should be an all-reject filter to suppressing the aliasing term $X(-z)$ and we assume the magnitude of $D(-z)I(z)$ should be smaller than -60dB. From above discussions, we design D and I as following. For $D(z)I(z)$ suppressing the image in $F_{39}(z^2)$, we set D and I 's stopband frequency = 0.628π and passband frequency = 0.374π (to cover the passband of F_{36}), as shown in Fig. 7. For $D(-z)I(z)$ suppressing $X(-z)$ to -60dB, we set D and I 's stopband attenuation = -60 dB, and we gradually decreased the stopband frequency (starting from 0.628π) until the magnitude of $D(-z)I(z)$ is smaller than -60 dB. Finally, the ripple of D and I is successively reduced until the ripples of $F_{22} \sim F_{36}$ are within 1 dB. This procedure leads to a 29-tap filter for D and a 34-tap filter for I .

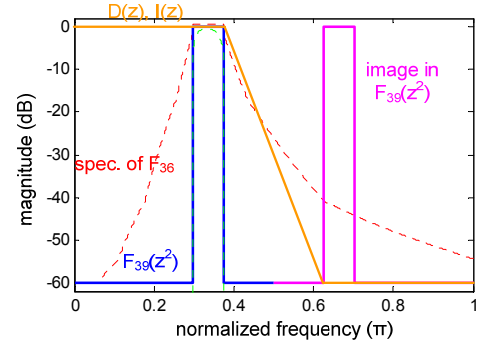


Figure 7. $F_{39}(z^2)$ and the specification of the 36th band

TABLE I FINE-TUNING RESULT

| ripple (dB) | | # taps | | | | | complexity | |
|-------------|-------------|-----------|-----------|-----------|-----------|-----------|------------|------------|
| F_{37-39} | D/I | F_{37} | F_{38} | F_{39} | D | I | # mpy | # add |
| 0.0 | 0.40 | - | - | - | 29 | 34 | NA | NA |
| 0.1 | 0.20 | 57 | 46 | 36 | 32 | 37 | 206 | 398 |
| 0.2 | 0.30 | 56 | 45 | 36 | 32 | 37 | 204 | 394 |
| 0.3 | 0.10 | 53 | 44 | 33 | 35 | 41 | 206 | 393 |
| 0.4 | 0.30 | 52 | 41 | 33 | 32 | 37 | 194 | 372 |
| 0.5 | 0.10 | 52 | 41 | 33 | 35 | 41 | 202 | 386 |
| 0.6 | 0.10 | 48 | 38 | 33 | 35 | 41 | 194 | 372 |
| 0.7 | 0.10 | 47 | 37 | 30 | 35 | 41 | 190 | 362 |
| 0.8 | 0.10 | 42 | 33 | 26 | 35 | 41 | 176 | 336 |
| 0.9 | 0.10 | 41 | 33 | 26 | 35 | 41 | 176 | 334 |
| 1.0 | 0.02 | 40 | 33 | 25 | 41 | 48 | 186 | 356 |

■ Step 2: Fine tuning

The ripple caused by $D(z)I(z)$ plus the ripple of $F_{37} \sim F_{39}$ could make the response of $F_{22} \sim F_{36}$ out of specifications. Therefore, the

filters need to be fine-tuned for the overall ripple. Since D and I are designed assuming $F_{37} \sim F_{39}$ has ripple = 0 dB. Here we gradually increase the ripple of $F_{37} \sim F_{39}$ and find out how small the ripple of D and I should be to make $F_{22} \sim F_{36}$ meet the specifications. We design $F_{37} \sim F_{39}$ with ripple = 0.1~1 dB and choose the best one. The results and the computations per sample are shown in Table I.

IV. RESULTS

A. Computational Complexity

To demonstrate the effectiveness of the multi-rate architecture and our proposed FIR optimizations, we have designed the parallel and the multi-rate FIR banks respectively for the 22nd ~ 39th band in ANSI 1/3-octave bands. We have also designed the parallel [9] and the multi-rate IIR [6] banks for comparison. The ANSI S1.11 implementations in the literatures [6][7][9] all adopted Butterworth IIR. In general, Elliptic IIR has smaller orders but the difference is small since the orders are both quite small. Thus, Butterworth is also used in this comparison. The input sampling rate is 24 kHz, which covers the 39th band. All filter coefficients are generated using the MATLAB (version 7.2) filter design toolbox. Table II summarizes the numbers of multiplications and additions for a single input sample. For parallel structure, the FIR bank requires filters of order 25 ~ 1,488, while the IIR one uses 8th-order Butterworth for F_{39} and 6th-order Butterworth for $F_{38} \sim F_{22}$ (F_n denotes the filter of the n th band). Therefore, the parallel FIR bank requires 3,270 multiplications (coefficient symmetry is exploited) and the parallel IIR bank requires 220 multiplications. In other words, the parallel FIR bank needs 14.8 times more multiplications than the IIR one. On the other hand, the multi-rate FIR bank implements 26/33/40-tap FIR filters $F_{37} \sim F_{39}$ respectively, and a 35-tap FIR filter for decimation. Thus, an input sample requires 135 multiplications and 257 additions respectively, which saves 96% computations in the parallel FIR bank. Note that the multi-rate architecture reduces the computation of the parallel IIR bank as well. However, the reduction is not as significant as the FIR bank and thus the multi-rate FIR bank has comparable complexity with the multi-rate IIR bank.

TABLE II COMPLEXITY COMPARISON

| | | IIR | FIR |
|------------|-------|-----|-------|
| Parallel | # mpy | 220 | 3,270 |
| | # add | 165 | 6,510 |
| Multi-rate | # mpy | 117 | 135 |
| | # add | 90 | 257 |

B. Filter Response

Fig. 8 shows the response of the 22nd band for the four filter banks. The ANSI S1.11 class-2 specifications are also plotted (the red and the green curves) to demonstrate the filter banks comply with the standard. We can see that the FIR bank adopts the equal ripple design, which requires a sharper slope in transition to meet the specification, while the response of IIR bank is smoother. Besides, an image component (the circled) is present in the response of multi-rate filter banks, as that we discussed in Section 3. The passband ripple of the multi-rate filter banks is slightly greater than that of the parallel filter banks; the reason is both the decimation and interpolation filters may add additional ripples to the response.

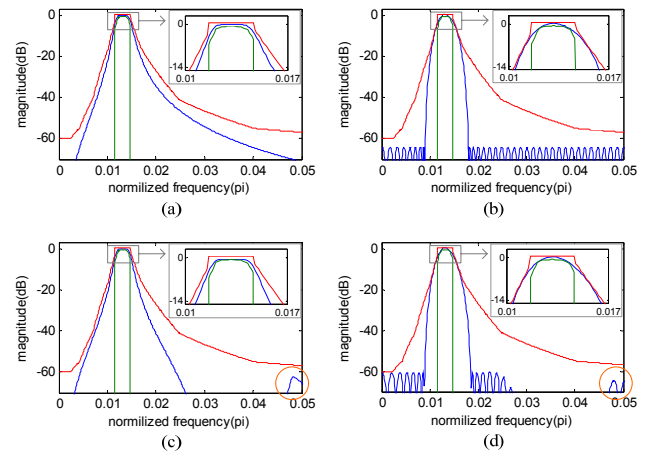


Figure 8. Response of the 22nd band in (a) parallel IIR bank (b) parallel FIR bank (c) multi-rate IIR bank and (d) multi-rate FIR bank

V. CONCLUSION

In this paper, we propose a multi-rate architecture to implement the ANSI S1.11 filter bank with FIR filters for digital hearing aids, where the computations can be greatly reduced with the multi-rate processing. We also propose a systematic flow to optimize the FIR coefficients for the multi-rate filter banks to minimize their orders. Our design saves 96% multiplications and additions of a parallel FIR bank. By the way, multi-rate processing can be applied on the IIR filter bank as well. However, the complexity reduction is not as significant as that of FIR banks. In brief, our multi-rate FIR bank has linear-phase property and also has comparable complexity with IIR banks. In the future, we will study the fixed-point coefficients with numerical optimizations to further reduce the implementation complexity of the FIR banks.

REFERENCES

- [1] H. Dillon, *Hearing Aids*, Thieme Medical Publisher, 2001
- [2] M. S. Ho and S. T. Young, "Building a platform of hearing aid's compensative strategy for Mandarin," in *Proc. International Congress on Acoustics*, 2004
- [3] *Specification for Octave-band and Fractional-octave-band Analog and Digital Filters*, ANSI S1.11-2004, Feb. 2004, Standards Secretariat Acoustical Society of America
- [4] K. S. Chong, B. H. Gwee and J. S. Chang, "A 16-channel low-power nonuniform spaced filter bank core for digital hearing aid," *IEEE Trans. Circuits Syst. II, Exp. Briefs*, vol. 53, Sept. 2006
- [5] Y. Lian and Y. Wei, "A computationally efficient nonuniform FIR digital filter bank for hearing aids," *IEEE Trans. Circuits Syst. I, Reg. Papers*, vol. 52, Dec. 2005
- [6] A. Lozano and A. Carlosena, "DSP-based implementation of an ANSI S1.11 acoustic analyzer," *IEEE Trans. Instrum. Meas.*, vol. 52, Aug. 2003
- [7] J. W. Waite, "A multirate bank of digital bandpass filters for acoustic applications – design of HP's 3569A real-time frequency analyzer," *Hewlett-Packard Journal*, Apr. 1993
- [8] P. P. Vaidyanathan, *Multirate Systems and Filter Banks*, Prentice Hall, 1993
- [9] P. Y. Lin, *Feasibility Study of the Implementation of Hearing Aid Signal Processing Algorithms on the TI TMS320C6713 DSK*, Master thesis, Institute of Biomedical Engineering, National Yang Ming University, 2004